19 May 1982

VLB ARRAY MEMO No. 84

A Design Study for a Dedicated VLBI Array

by

R. L. MUTEL and R. A. GAUME

Department of Physics and Astronomy
The University of Iowa
Iowa City, Iowa 52242

February 1982

ABSTRACT

A design study of the optimal locations for a ten-station array of radio telescopes, using earth-rotation synthesis, has been performed. The algorithm used a weighted circular grid of points in the transfer function plane. Thirteen arrays of ten stations each were analyzed over a range of nine source declinations from -44° to +64°. The results show that there exist many arrays which provide good coverage for northern declinations but which are poor at southerly declinations. The exact location of an array element is generally not critical and can be moved by at least 100 km without significantly affecting overall coverage. The replacement of one or two northern hemisphere elements with southern hemisphere stations (for example, Galapagos Islands and/or Easter Island) dramatically improves (u,v) plane coverage at all declinations below +30° declination, or about three-fourths of the celestial sphere.

1.0 INTRODUCTION

There is now a worldwide network of radio observatories that regularly schedule joint experiments using the technique of very long baseline interferometry (VLBI). This technique allows astronomers to probe the structure of galactic and extragalactic radio sources with the angular resolution of order 10^{-3} arcsec (1 mas), far greater than observations using any other technique.

Currently, there are six U. S. observatories who regularly schedule such observations (Hat Creek, University of California, Berkeley; Owens Valley Radio Observatory, Cal Tech; Harvard Radio Astronomy Station, Harvard; North Liberty Radio Observatory, University of Iowa; Haystack Observatory, M.I.T.; and the National Radio Astronqmy Observatory). This U. S. VLBI Network, as it is called, has an established procedure for submission of proposals and regular scheduling of observations. During the past few years, these observations have produced many important scientific advances such as detailed maps of 'superluminal' extragalactic sources and proper motion studies of H_2O masers in star-formation regions. Recent successful VLBI observations at 43 GHz and 90 GHz demonstrate very short wavelengths can be used, dramatically increasing the angular resolution. This will allow investigations which can probe near or at the dimensions of the central 'engine' itself.

There are several fundamental problems with current VLBI observations in that the telescopes vary widely in their performance (especially at short wavelengths) and their availability. Furthermore, the telescopes are not optimally placed for forming a 'clean' beam using earth rotation synthesis. Finally, the number of telescopes normally available (approximately five or six) is generally inadequate to produce maps with sufficient dynamic range to reliably detect weak or complex structures. These deficiencies have prompted several groups to suggest construction of a dedicated array of approximately ten new radio telescopes placed at optimal geographic locations. In this report we analyze the problem of optimization of the array element locations and suggest a class of array, including two elements in the southern hemisphere, which dramatically improve the synthesized beam at low source declinations.

2.0 ARRAY CONFIGURATION STUDIES

Previous studies of the problem of optimal array element locations have analyzed both the image plane and transfer function (u,v) plane. The former method was used in preliminary reports on a dedicated VLB array by groups at Cal Tech and NRAO. One advantage of image plane analysis is that the 'figure of merit' for comparison among different arrays is the dynamic range of the restored image, a directly interpreted quantity. A serious disadvantage, however, is that any given test image will have a non-uniform two dimensional spatial spectrum which may favor certain array configurations which happen to be sensitive to the test image's spatial spectrum. One can devise test sources with uniform spatial spectra over the prescribed resolution range of the array but a more direct (and computationally simpler) method is to analyze the transfer plane itself. We have chosen the latter method.

Previous studies using transfer plane algorithms have been restricted to optimization of arrays with fewer elements or with some locations fixed. The algorithm itself, however, is similar to those of Phillips and Mutel (1977), Swenson (1977), and Seielstad et al. (1980).

2.1 The Algorithm for Calculating the Array Figure of Merit

The algorithm consists of gridding the transfer (u,v) plane into a matrix of uniformly spaced grid points spaced at the minimum required baseline length and computing the distance from each grid point to the nearest (u,v) point using the given array. The u,v distances are then squared and summed for all points in the grid. This procedure is repeated for a series of 'standard' declinations chosen so that each declination line is centered on an annular strip of equal area on the celestial sphere. Since the angular resolution is inversely proportional to spatial frequency (approximately baseline length), an inverse radial weighting (R^{-1}) was applied to each term in the sum. The 'u-v' tracks, i.e., the (u,v) plane coverage for each baseline using earth-rotation synthesis, were computed as discrete points using a given integration time per unit. The grand 'figure of merit' for an array is the sum over declination of the individual sums for each declination. The figure of merit, being a measure of the 'holes' in the transfer plane coverage, is inversely proportional to the effective dynamic range of a 'uniform' source brightness (as discussed above).

We have convected the computer figures of merit to dynamic range by taking the reciprocal and scaling by a factor which forces agreement with the actual dynamic ranges computed for a sample source using the D-2 and CIT-13 arrays.

The range of grid points to be analyzed depends on the design resolution of the array. Since a rectangular grid arbitrarily favors (u,v) coverage along certain position angles (~ ± 45° and ± 135°), a circular boundary was chosen with the maximum baseline length as radius. Furthermore, we used the same circle for computations at all declinations, in spite of the well-known fact that continental U. S. baselines give highly flattened (u,v) tracks at low declinations. To compensate for this with elliptical boundaries, for example, would unfairly bias the analysis toward higher declination coverage.

2.2 Array Design Parameters

We chose the following values for the parameters discussed above:

Grid Spacing:	100 km
Radius of Grid Circle:	6000 km
Integration Time per (u,v) Point:	5 min
Number of Stations:	9 or 10
Declinations:	-44, -30, -18, -6, +6, +18, +30, +44, +64

2.3 Computational Considerations

The algorithm is very computer-intensive. A typical analysis of a single ten station array at all nine declinations with the above parameters took about 1½ hours of CPU time on a VAX 11/780 computer. The program used to calculate the (u,v) tracks was adopted from the program HAZI, which is part of the Cal Tech VLBI software package. The final program, called DAZI, is executable on a VAX computer and is available from the authors as a listing or on tape.

3.0 RESULTS

We have analyzed thirteen ten-station arrays including CIT-13 (Cal Tech study) and D-2 (NRAO study). The location of the stations for each array is tabulated in Table 1. The effective dynamic range for each array as a function of declination is plotted (Figures 1 and 2) and is tabulated in Table 2. In addition, in Figure 3 we have plotted the actual (u,v) plane coverage for array SEG-1 and for D-2 at four representative declinations (+44°, 6°, -30°, -44°). The dashed circle on each plot indicates the radius 6000 km within which the analysis was made.

There are two clear results of the analysis. First, for arrays which are located entirely on U. S. soil (including Puerto Rico), there are a large number with about the same overall dynamic range (D-2, CIT-13, N-1 -- N-7). This implies that the precise location of any single array element is unimportant to an uncertainty of at least one grid cell spacing ($\geq$ 100 km) and probably larger. An exception is the location of array elements on the shortest spacings since inverse radial weighting makes the location of those elements critical. In general, however, it appears that locations can be chosen to favor existing sites, nearby airports, etc., where appropriate.

The second result is that continental U. S. arrays all give very poor coverage at low declinations, but that the replacement of only two array elements with southern hemisphere locations can dramatically improve the total array response. This is clearly seen in both the dynamic range plots (Figures 2 and 3) and in the (u,v) tracks shown in Figure 4 which compare a good U. S. 'only' array with an eight-station element U. S. array plus elements in the Galapagos Islands and Easter Island. The southern array (denoted SEG-1 in this report) is better than CIT-13 at <u>all</u> declinations less than +30°, i.e., in 75% of the total celestial sphere. The difference is even more striking when galactic plane studies are considered, since almost all of the galactic disk interior to the sun is below +30° declination. The differences are very great at low declinations; for example, the CIT-13 array is very nearly one dimensional at -30° (near the galactic center), whereas the SEG-1 array has excellent two dimensional coverage and contains more than 1.5 times as many points.

3.1 Alternative 'Southern' Arrays

The locations of the two southern hemisphere elements is critical -- there appear to be no other nearby alternatives. The entire South American mainland is too far to the east relative to the North American continent to give uniform two-dimensional coverage. (The tracks are 'tilted' along p.a. ~ 45° and give poor coverage along -45°.) Stations in Tahiti, New Zealand, Pitcairn Island, etc. are all much too far west and also give 'tilted' arrays.

We have also investigated the possibility of adding only a single southern hemisphere station (in case either the Galapagos Islands or Easter Island locations present insurmountable problems). The resulting arrays are labeled SG-1 and SE-1, respectively, and are included in Figures 2 and 3. Note that in each case the continental U. S. stations were readjusted to optimize the entire array. This was done by trial-and-error and it is likely that the arrays could be improved further.

Inspection of figures and companion tables indicates that the Galapagos Islands site is substantially more important than the Easter Island site for arrays containing only one southern hemisphere station. The overall dynamic range for the SG-1 array is 86% that of the SEG-1 array, while the SE-2 array (Easter Island only) gives an average or 74% that of the SEG-1 array. Arrays containing either site, however, give substantially better (u,v) plane coverage than any northern hemisphere array.

APPENDIX

Geopolitical Data for Galapagos and Easter Islands

A. Galapagos Islands (Ecuador)

Location: 91° W, -2° S; 650 miles west of Ecuador

Size: 3,029 mi^2 (13 large islands)

Population: 3000 (estimate, 1970)

Topography: Mostly lava, dense vegetation on upper slopes; volcanic mountains up to 5000 feet

Logistics: Regular air service from Quito to Isabela (largest island)

Other: During World War II, U. S. maintained an air base there; since abandoned. There has been a satellite tracking station there since 1967.

B. Easter Island (Chile)

Location: 109° W, 27° S; 2200 miles west of Chile

Size: 46 square miles

Population: 1600 (estimate, 1970)

Topography: Mostly low-lying grasslands

Other: Chile has declared the island a historical monument. The optical facility CTIO (   ) has been operated on Chilean soil since   and could provide a useful comparison for cost and logistics projections. In 1981 the average costs of on-site staff at CTIO and KPNO was about the same.

Location	Abbreviation	Latitude	Longitude
Anchorage, Alaska	ANCH	61.0	150.0
Arecibo, Puerto Rico	ARECIBO	18.3	66.8
Big Pine, California	OVRO	37.0	118.3
Bismarck, North Dakota	BSMK	47.0	101.0
Boise, Idaho	BOISE	42.7	116.0
Boulder, Colorado	BLDR	40.0	105.3
Brownsville, Texas	BRVL	26.0	97.4
Colorado Springs, Colorado	COSPR	38.8	104.9
Easter Island	EASTER	-27.0	109.0
Fort Irwin, California	DSS13	35.1	116.8
Galapagos Islands	GAL	- 0.9	89.5
Grand Forks, North Dakota	GFRK	47.9	97.2
Green Bank, West Virginia	NRAO	38.3	79.8
Hawaii	HAW	19.8	155.5
Honolulu, Hawaii	HNLU	21.3	157.8
Ketchikan, Alaska	KECH	55.5	131.5
Laramie, Wyoming	LARA	41.2	105.6
Laredo, Texas	LRDO	27.5	99.0
Las Cruces, New Mexico	LASC	32.4	107.0
Miami, Florida	MIAMI	26.0	81.0
New Orleans, Louisiana	NWOR	30.0	90.0
North Liberty, Iowa	IOWA	41.6	91.6
Phoenix, Arizona	PHNX	33.4	112.0
Salem, Oregon	SALEM	45.0	123.0
Sante Fe, New Mexico	SAFE	35.6	105.9
Sioux Falls, South Dakota	SUFL	43.5	96.7
Socorro, New Mexico	VLA	34.1	107.6
Tucson, Arizona	TUCSON	32.4	111.0
Westford, Massachusetts	HSTK	42.4	71.5
West Coast, Ecuador	QITW	0.0	80.0
Quito, Ecuador	QITO	0.2	78.5

ARRAY	STATIONS				
D-2	HSTK	OVRO	ANCH	HNLU	VLA
	SAFE	BLDR	GFRK	BRVL	NRAO
CIT-13	HSTK	OVRO	ANCH	HNLU	IOWA
	LRDO	BLDR	BOISE	DSS13	SALEM
N-1	HSTK	OVRO	ANCH	HAW	VLA
	TUCSON	LARA	AREBICO	KECH	SUFL
N-2	HSTK	OVRO	ANCH	HAW	VLA
	BOISE	LASC	ARECIBO	IOWA	MIAMI
N-3	HSTK	OVRO	ANCH	HAW	VLA
	COSPR	LARA	ARECIBO	GFRK	MIAMI
N-4	HSTK	OVRO	ANCH	HAW	LASC
	COSPR	LARA	ARECIBO	GFRK	NWOR
N-5	HSTK	OVRO	ANCH	HAW	VLA
	COSPR	LARA	ARECIBO	LRDO	MIAMI
N-6	HSTK	OVRO	ANCH	HNLU	VLA
	PHNX	LARA	ARECIBO	KECH	SUFL
N-7	HSTK	OVRO	ANCH	HNLU	VLA
	LASC	BLDR	ARECIBO	SUFL	KECH
SG-1	HSTK	OVRO	SALEM	HAW	VLA
	TUCSON	BRVL	ARECIBO	GAL	BSMK
SE-1	HSTK	OVRO	EASTER	HAW	VLA
	TUCSON	BRVL	ARECIBO	ANCH	BSMK
SEG-1	HSTK	OVRO	EASTER	HAW	VLA
	TUCSON	BRVL	ARECIBO	GAL	BSMK
SEG-2	NRAO	OVRO	EASTER	HAW	VLA
	TUCSON	BRVL	ARECIBO	GAL	BSMK
SQ-1	HSTK	OVRO	SALEM	HAW	VLA
	TUCSON	BRVL	ARECIBO	QITW	BSMK
SQ-2	HSTK	OVRO	SALEM	HAW	VLA
	TUCSON	BRVL	ARECIBO	QITO	BSMK

Table 1. Dynamic Range of Thirteen Ten-Station Arrays

Array	D-2	CIT-13	N-1	N-2	N-3	N-4	N-5	N-6	N-7	SE-1	SG-1	SEG-1	SEG-2
Dec 64°	537	461	542	409	502	487	487	547	507	479	503	426	412
44°	423	366	379	355	370	394	384	372	351	353	384	314	297
30°	269	241	287	292	292	251	304	276	274	262	314	257	253
18°	269	149	198	198	198	194	206	180	176	210	262	216	210
6°	106	106	120	125	128	127	123	110	111	148	179	166	171
-6°	77	74	84	84	86	86	82	76	77	121	145	149	151
-18°	50	51	61	60	60	62	59	57	52	93	134	156	146
-30°	50	34	43	45	43	44	45	41	41	72	94	140	139
-44°	18	19	21	25	23	22	27	21	14	45	45	68	68
Total	63	64	75	79	78	77	82	72	61	119	139	163	161
Total (excluding -44°)	93	81	109	110	110	111	111	103	102	150	189	198	115

Table 2. Dynamic Range of Thirteen Ten-Station Arrays Normalized to SEG-2 Array

Array	D-2	CIT-13	N-1	N-2	N-3	N-4	N-5	N-6	N-7	SE-1	SG-1	SEG-1	SEG-2
Dec 64°	131	112	132	100	122	118	111	133	123	117	122	104	100
44°	142	124	128	119	125	133	130	126	118	119	129	106	100
30°	106	95	113	115	115	99	120	109	108	104	124	102	100
18°	77	71	94	95	94	92	98	86	84	100	124	103	100
6°	62	62	70	73	75	74	72	64	65	86	105	97	100
-6°	51	49	56	56	57	57	55	50	51	80	96	99	100
-18°	34	35	41	41	41	42	41	39	39	64	92	106	100
-30°	24	25	31	33	31	32	33	30	30	52	68	101	100
-44°	26	28	31	36	34	33	39	31	21	67	66	100	100
Total	39	40	46	49	48	48	51	44	38	74	86	101	100
Total (excluding -44°)	48	47	56	56	57	57	57	53	53	77	97	102	100

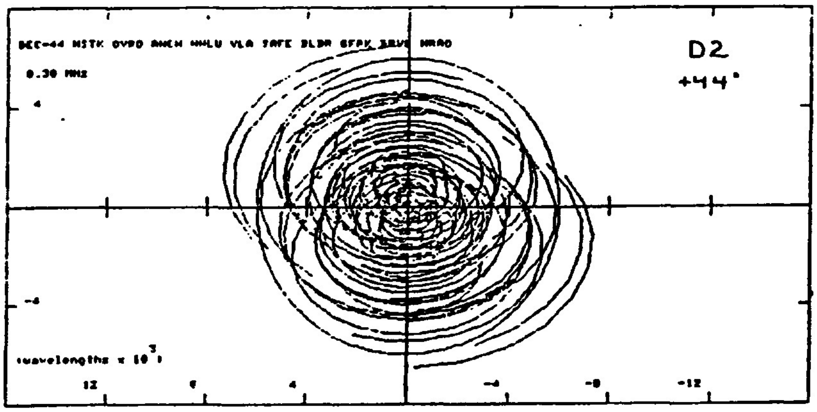
DEC=44 NSTK OVRO ANCH HHLU VLA TAFE BLDR GFPK BRVL HRAO
0.30 MHz
4
-4
(wavelengths x 10^3)
12
8
4
-4
-8
-12
D2
+44°

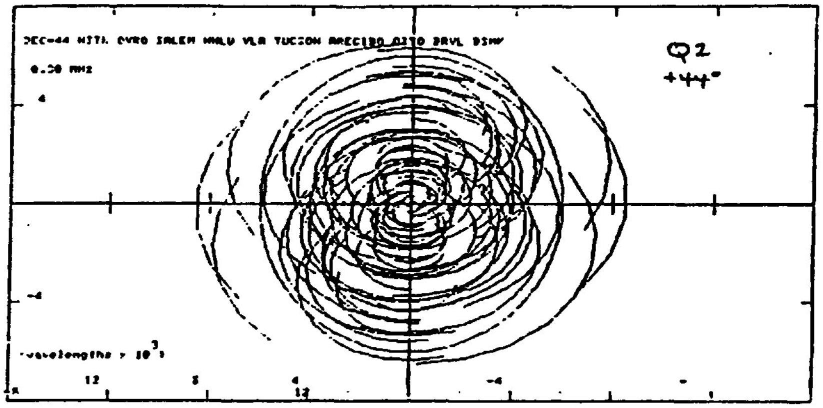
DEC=44 NSTK OVRO SALEM HHLU VLA TUCSON ARECIBO AUTO BRVL DSHV
0.30 MHz
4
-4
(wavelengths x 10^3)
12
8
4
-4
Q2
+44°

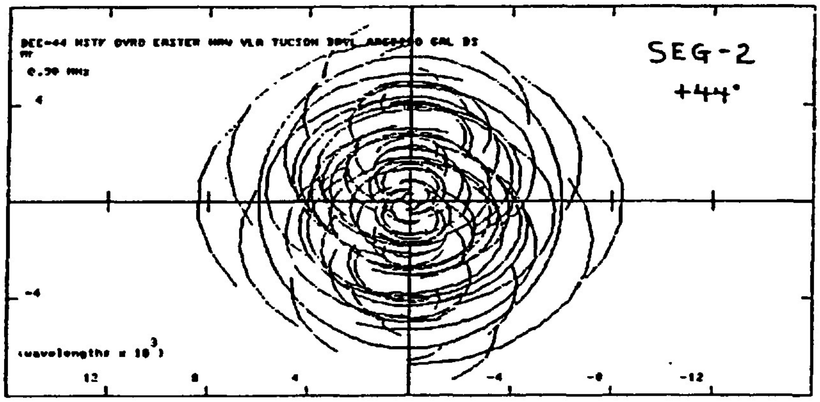
DEC=44 NSTF OVRO EASTER HAW VLA TUCSON BRVL ARECIBO GAL DS
0.30 MHz
4
-4
(wavelengths x 10^3)
12
8
4
-4
-8
-12
SEG-2
+44°

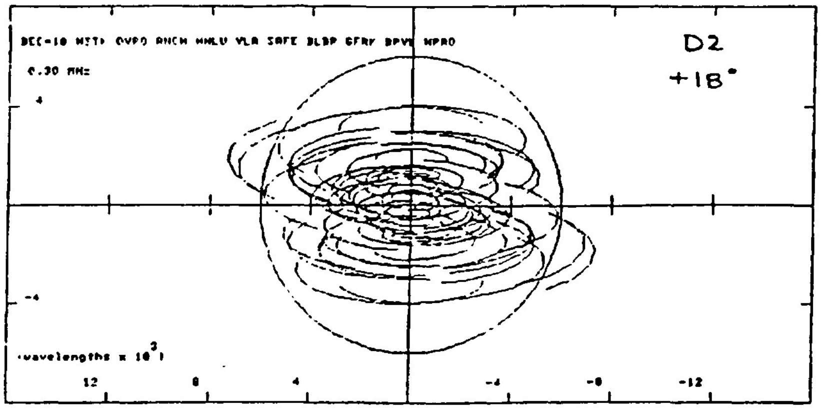

D2
+18°

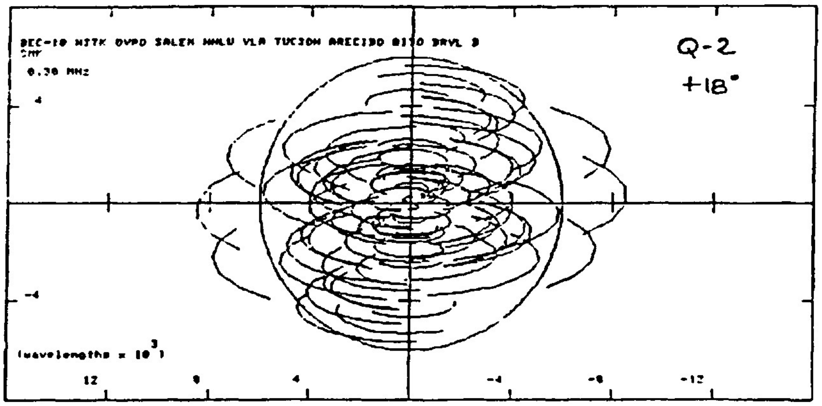

Q-2
+18°

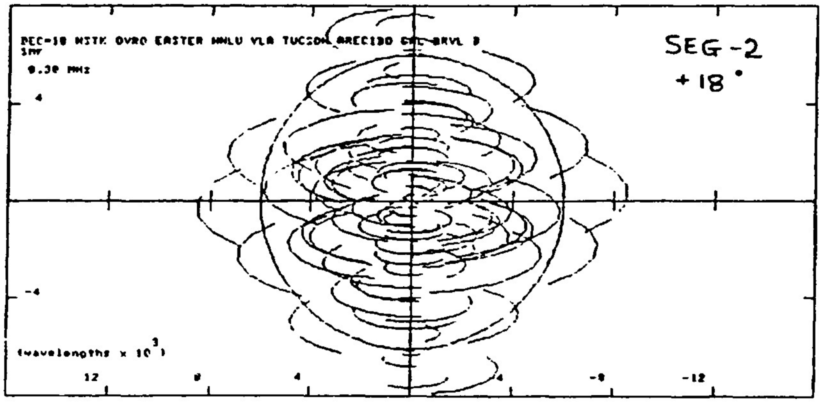

SEG-2
+18°

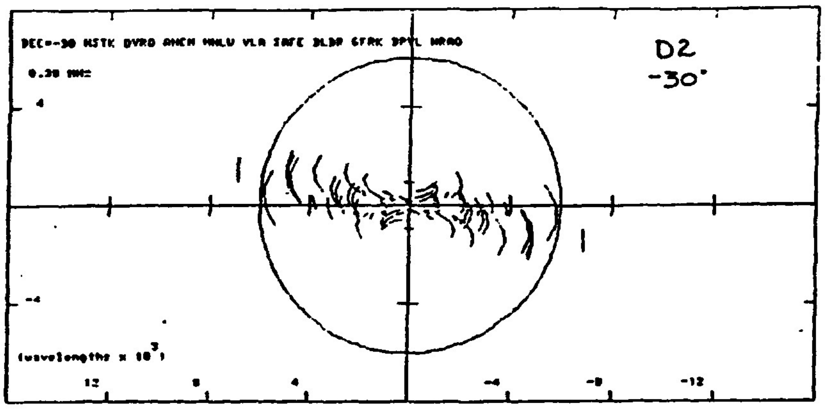
DEC=-30 HSTK OVRO ANCH MNLU VLA SAFE BLDR GTRK DPYL NRAO
0.30 MHz
4
-4
(wavelengths x 10^3)
12
8
4
-4
-8
-12
D2
-30°

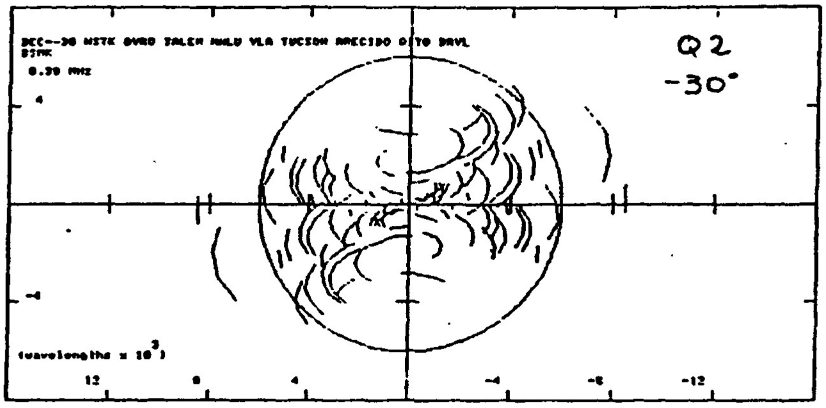
DEC=-30 HSTK OVRO SALEM MNLU VLA TUCSON ARECIBO GOTO BRVL
BSNK
0.30 MHz
4
-4
(wavelengths x 10^3)
12
8
4
-4
-8
-12
Q2
-30°

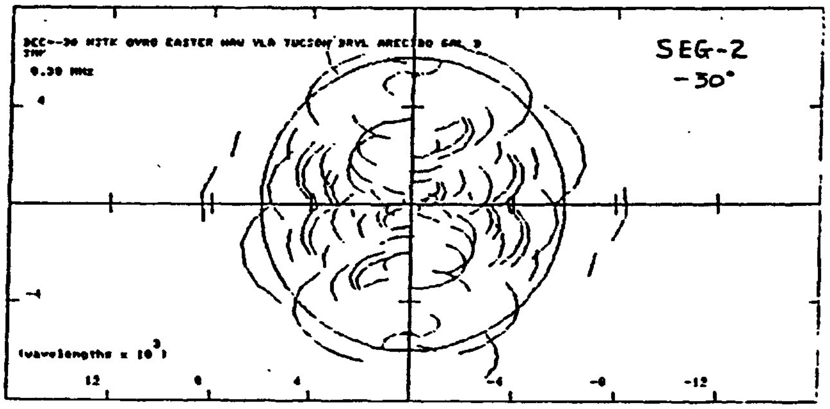
DEC=-30 HSTK OVRO EASTER HAW VLA TUCSON BRVL ARECIBO GAL 9
SNP
0.30 MHz
4
-4
(wavelengths x 10^3)
12
8
4
-4
-8
-12
SEG-2
-30°

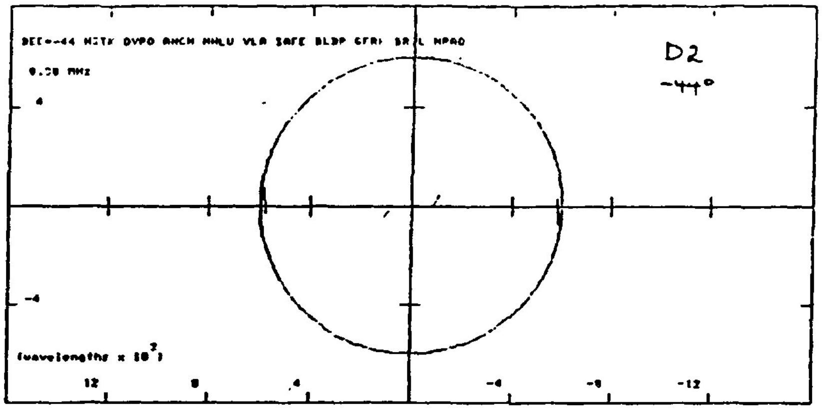
DEC=-44 HSTK OVRO ANCH MHLU VLA SAFE BLBP GFRI BRXL NPAO
0.30 MHz
D2
-44°
4
-4
(wavelengths x 10^3)
12
8
4
-4
-8
-12

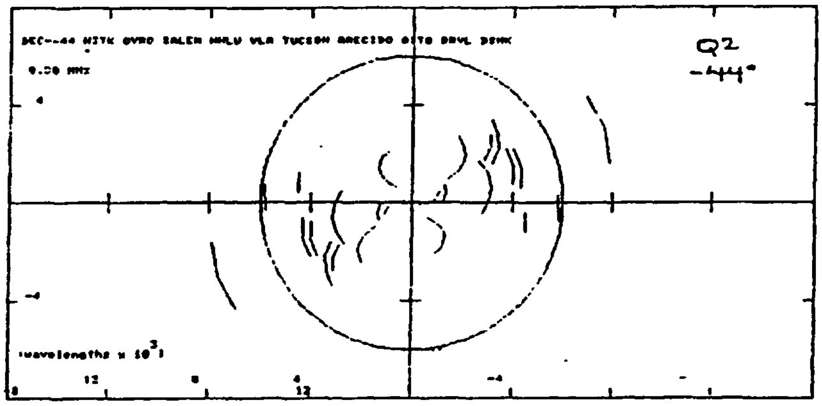
DEC=-44 HSTK OVRO SALEM MHLU VLA TUCSON ARECIBO ALTO BRVL DSMK
0.30 MHz
Q2
-44°
4
-4
(wavelengths x 10^3)
12
8
4
-4

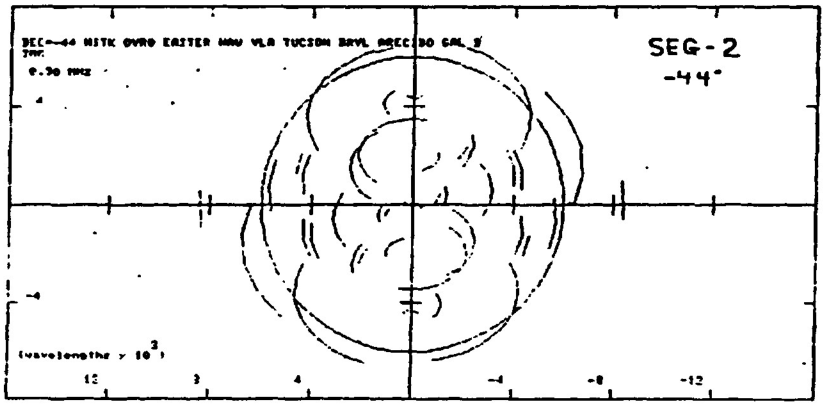
DEC=-44 HSTK OVRO EASTER HAW VLA TUCSON BRVL ARECIBO GAL 3
0.30 MHz
SEG-2
-44°
4
-4
(wavelengths x 10^3)
12
8
4
-4
-8
-12